Supplemental Material: Quantum Approach to Fast Protein-Folding Time

Li-Hua Lu (吕丽花)[1] and You-Quan Li(李有泉)[1,2,*]

[1] *Zhejiang Province Key Laboratory of Quantum Technology & Device and Department of Physics, Zhejiang University, Hangzhou 310027, P.R. China.*

[2] *Collaborative Innovation Center of Advanced Microstructure, Nanjing University, Nanjing 210008, R.R. China.*

I. METHODS

For $n = 4$, the structure set consists of 4 objects and the connection graph defined by the one-step folding is just a three-star graph (see Fig. 1(b)). There are totally 16 possible sequences in the sequence set $\Omega_4 = \{[1],[2],\cdots,[16]\}$ (see Table SI for details) This sequence set is partitioned into three subsets, *i.e.*, $\Omega_4 = \{Q_1, Q_2, Q_3\}$ with $Q_1 = \{[1],[3],[5],[7]\}$, $Q_2 = \{[2],[4],[6],[8],[9],[11],[13],[15]\}$ and $Q_3 = \{[10],[12],[14],[16]\}$. Their corresponding potential energies $(\mathcal{E}_1, \mathcal{E}_2, \mathcal{E}_3, \mathcal{E}_4)$ are calculated as $(0,0,0,0)$, $(0,0,0,-1)$ and $(0,0,0,-2.3)$ respectively. Thus there will be three situations in the discussion on the time evolution. For the classical random walk on graph $\mathcal{G}_4$, we have

$$\tilde{K} = \begin{pmatrix} -1 & 1/3 & 0 & 0 \\ 1 & -1 & 1 & 1-\Omega \\ 0 & 1/3 & -1 & 0 \\ 0 & 1/3 & 0 & -1+\Omega \end{pmatrix},$$

where $\Omega = (\mathcal{E}_4)^2/\big[(\mathcal{E}_4)^2+1\big]$ with the contact energy $\mathcal{E}_4 = 0$, -1, and -2.3 respectively for Q_1, Q_2 and Q_3 cases. For each case we solve the equation (4) with the initial condition $p_a(0) = \delta_{a,1}$ and $p_a(0) = \delta_{a,4}$, respectively, and get the time evolution of $p_a^{(1)}(t)$ and $p_a^{(4)}(t)$ where the superscript is used to distinguish the solutions with different initial conditions.

A. The density matrices

The quantum walk on a graph $\mathcal{G}_n$ is described by the time evolution of a density matrix that is governed by the matrix equation (6) of the main textwhere the Hamiltonian $\hat{H}^{[\nu]}$ is of sequence $[\nu]$ dependent. As an example, we first illustrate the case of $n = 4$, for which the Hamiltonian reads

$$\hat{H}^{[\nu]} = \begin{pmatrix} 0 & -1 & 0 & 0 \\ -1 & 0 & -1 & -1 \\ 0 & -1 & 0 & 0 \\ 0 & -1 & 0 & \mathcal{E}_4^{[\nu]} \end{pmatrix}, \tag{1}$$

where $\mathcal{E}_4^{[\nu]} = 0$ for the sequences in the subset Q_1, $\mathcal{E}_4^{[\nu]} = -1$ for those in Q_2, and $\mathcal{E}_4^{[\nu]} = -2.3$ for those in Q_3. For each case, we substitute Eq. (1) into Eq. (6) of the main text to determine the time evolution of the 4 by 4 density matrix $\hat{\rho}(t) = \{\rho_{a,b}(t) \mid a,b = 1,2,3,4\}$. In our numerical calculation, we set $\hbar$ and J to be unity and take the time step as $\Delta t = 0.02$. For the initial condition, $\rho_{11}(0) = 1$ and the other matrix elements vanish when $t = 0$, we solve the aforementioned first-order differential equation (6) of the main text by means of Runge-Kutta method and obtain the magnitudes of $\rho_{ab}^{(1)}(t)$ at any later time, $t = j * \Delta t$ with $j = 1,2,\cdots$.

In order to have an intuitive picture we plot in Fig. S2 the density matrix at a certain time t when $\rho_{4,4}^{(1)}(t)$ first reaches its maximum value. The off-diagonal elements of density matrix in quantum mechanics are usually complex numbers, so we use histogram heights to evaluate the modules and colors to label the phases of the complex numbers. The time dependence of the diagonal element of the solved density matrix for the Q_3 case is plotted in Fig. 2 for an intuitive illustration. Likewise, we need to solve the density matrix for another initial condition, $\rho_{44}(0) = 1$ again so that the first-passage probability can be determined.

Similarly, the study of the quantum walk on the graph $\mathcal{G}_6$ is a task to solve the 22 by 22 density matrix from Eq. (6) of the main text for the forty-five situations (see Table SIII) one by one. Here the potential term in the total Hamiltonian is expressed as $V = \sum_{a=1}^{22} \mathcal{E}_a \mid a\rangle\langle a \mid$ with $\mathcal{E}_a \neq 0$ for $a = 4,8,9,10,16,17,18,19$ and 20 while $\mathcal{E}_a = 0$ for $a = 1,2,3,5,6,7,11,12,13,14,15,21$ and 22. In terms the solved density matrices we can calculate the fist-passage probability furthermore.

B. The first-passage probabilities

For numerical calculation, the discrete version of Eq. (8) is given by

$$F_{14}(k*\Delta t) = \frac{P_{1,4}(k*\Delta t)}{\Delta t} - \sum_{l=0}^{k-1} F_{1,4}\big(l*\Delta t\big)P_{4,4}\big((k-l)*\Delta t\big), \tag{2}$$

with $k = 1,2,\cdots$. As we have $P_{1,4}(i*\Delta t) = \rho_{44}^{(1)}(i*\Delta t)$, $P_{4,4}(i*\Delta t) = \rho_{44}^{(4)}(i*\Delta t)$ together with the natural initial conditions $F_{1,4}(0) = 0$, $P_{1,4}(0) = 0$ and $P_{4,4}(0) = 1$, the above relation (2) for $k = 1$ gives rise to $F_{1,4}(\Delta t) = P_{1,4}(\Delta t)/\Delta t$, and furthermore for $k = 2,\cdots$ iteratively gives rise to $F_{1,4}(k*\Delta t)$. Since $F_{1,4}(k*\Delta t)$ oscillates with time, when $F_{1,4}(k*\Delta t)$ first appears to be negative

* email: yqli@zju.edu.cn

value, we record the corresponding value of k as k_0. This implies that the upper limit of integration τ_0 in Eq. (9) of the main text is between the value of $(k_0-1)*\Delta t$ and $k_0*\Delta t$. In our calculation of the folding time, we take $\tau_0 \approx (k_0-1)*\Delta t$ in the discrete version of the formula (9) consequently,

$$\tau_{\rm fd} = \frac{\sum_{k=1}^{k_0-1} k*\Delta t * F_{1,4}(k*\Delta t)*\Delta t}{\sum_{k=1}^{k_0-1} F_{1,4}(k*\Delta t)*\Delta t}. \qquad (3)$$

We calculated the folding times numerically for each case, our results are listed in the Tables SIV, SV and SVI.

II. SUPPLEMENTAL FIGURES AND TABLES

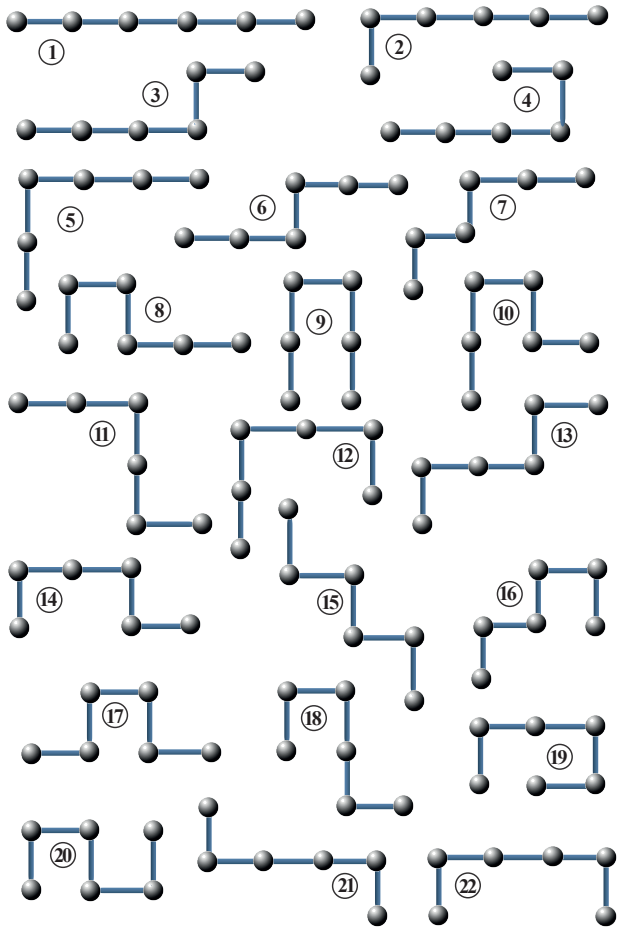

FIG. S1. The contents of the structure set $\mathcal{S}_6$. There are twenty-two distinct structures for the amino-acid chain with six residues (the case of n=6). Here the structures numbered as 9, as 19, and as 20 are called the most compact structures. The contact energy $\mathcal{E}_a \neq 0$ for the structure-a with $a = 4, 8, 9, 10, 16, 17, 18, 19$ and 20, while $\mathcal{E}_a = 0$ for the other structures.

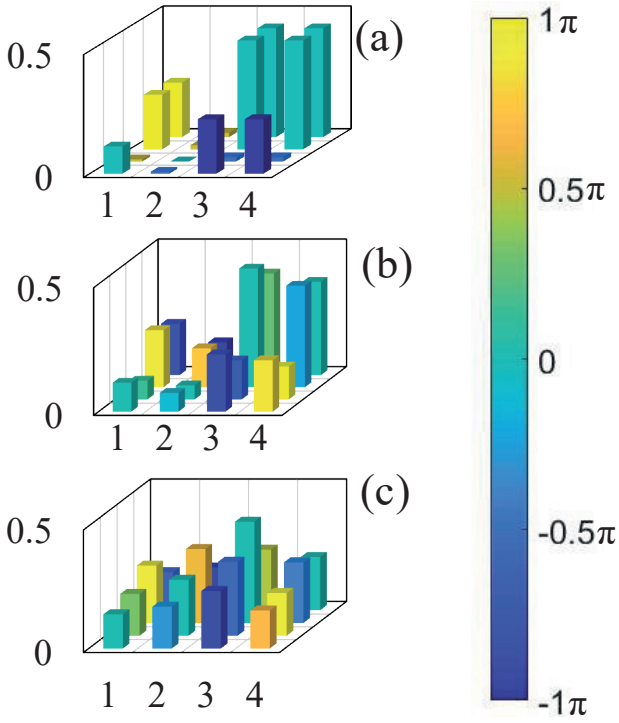

FIG. S2. Color histogram of the density matrix. The solved density matrix at the first time when $\rho_{44}^{(1)}$ reaches its maximum value is plotted in terms of colored histogram, in which the heights evaluate the modules of the matrix element and the colors measured in the color-bar present their complex-number phases. We plotted density matrices, respectively from the solutions, (a) for the subset Q_1 at $t = 1.82$, (b) for Q_2 at $t = 1.70$ and (c) for Q_3 at $t = 1.52$. Clearly, the existence of off-diagonal elements reflects the quantum coherence that speeds up the protein folding process.

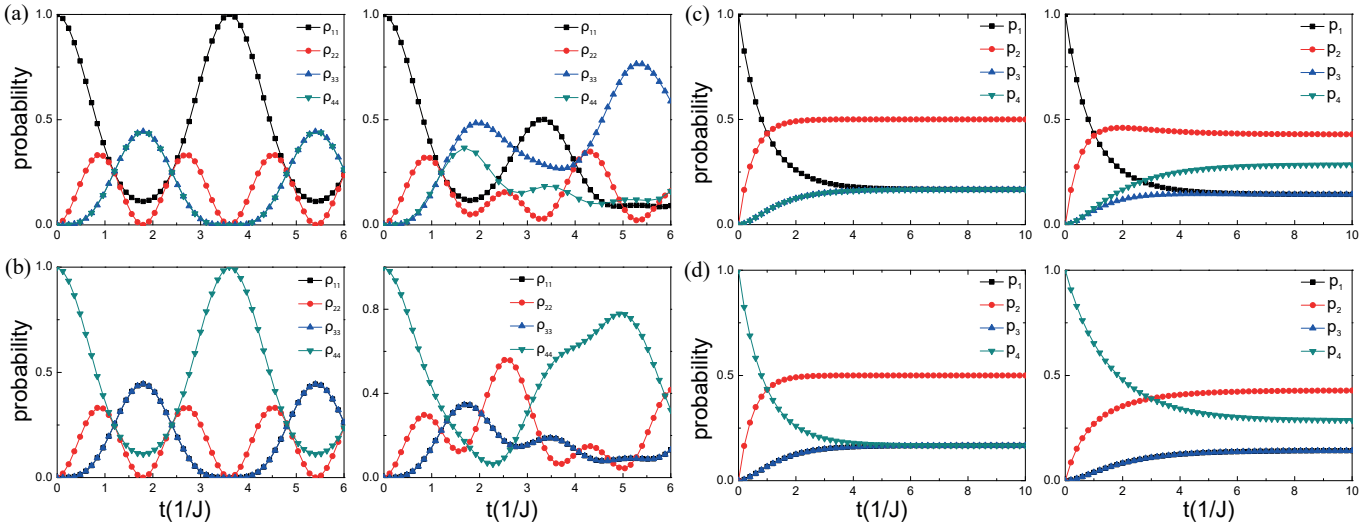

FIG. S3. The evolution of quantum and classical probabilities. The time dependence of the diagonal elements of the quantum mechanical density matrix and the corresponding classical counterparts for the other two sequence subsets Q_1 (left panel) and Q_2 (right panel). The diagonal elements of the density matrix solved from the initial conditions (a) $\rho(0) = \mid s_1 \rangle\langle s_1 \mid$ and (b) $\rho(0) = \mid s_4 \rangle\langle s_4 \mid$. The corresponding classical solutions of the probability distribution solved from two initial conditions (c) $p_b(0) = \delta_{b1}$ and (d) $p_b(0) = \delta_{b4}$.

TABLE SI. The collection of sequences in the sequence set $\mathcal{Q}_4$

$[1] = (P,P,P,P)$	$[2] = (P,P,P,H)$	$[3] = (P,P,H,P)$	$[4] = (P,P,H,H)$
$[5] = (P,H,P,P)$	$[6] = (P,H,P,H)$	$[7] = (P,H,H,P)$	$[8] = (P,H,H,H)$
$[9] = (H,P,P,P)$	$[10] = (H,P,P,H)$	$[11] = (H,P,H,P)$	$[12] = (H,P,H,H)$
$[13] = (H,H,P,P)$	$[14] = (H,H,P,H)$	$[15] = (H,H,H,P)$	$[16] = (H,H,H,H)$

TABLE SII. The collection of sequences in the sequence set $\mathcal{Q}_6$

$[1]=(P,P,P,P,P,P)$	$[2]=(P,P,P,P,P,H)$	$[3]=(P,P,P,P,H,P)$
$[4]=(P,P,P,P,H,H)$	$[5]=(P,P,P,H,P,P)$	$[6]=(P,P,P,H,P,H)$
$[7]=(P,P,P,H,H,P)$	$[8]=(P,P,P,H,H,H)$	$[9]=(P,P,H,P,P,P)$
$[10]=(P,P,H,P,P,H)$	$[11]=(P,P,H,P,H,P)$	$[12]=(P,P,H,P,H,H)$
$[13]=(P,P,H,H,P,P)$	$[14]=(P,P,H,H,P,H)$	$[15]=(P,P,H,H,H,P)$
$[16]=(P,P,H,H,H,H)$	$[17]=(P,H,P,P,P,P)$	$[18]=(P,H,P,P,P,H)$
$[19]=(P,H,P,P,H,P)$	$[20]=(P,H,P,P,H,H)$	$[21]=(P,H,P,H,P,P)$
$[22]=(P,H,P,H,P,H)$	$[23]=(P,H,P,H,H,P)$	$[24]=(P,H,P,H,H,H)$
$[25]=(P,H,H,P,P,P)$	$[26]=(P,H,H,P,P,H)$	$[27]=(P,H,H,P,H,P)$
$[28]=(P,H,H,P,H,H)$	$[29]=(P,H,H,H,P,P)$	$[30]=(P,H,H,H,P,H)$
$[31]=(P,H,H,H,H,P)$	$[32]=(P,H,H,H,H,H)$	$[33]=(H,P,P,P,P,P)$
$[34]=(H,P,P,P,P,H)$	$[35]=(H,P,P,P,H,P)$	$[36]=(H,P,P,P,H,H)$
$[37]=(H,P,P,H,P,P)$	$[38]=(H,P,P,H,P,H)$	$[39]=(H,P,P,H,H,P)$
$[40]=(H,P,P,H,H,H)$	$[41]=(H,P,H,P,P,P)$	$[42]=(H,P,H,P,P,H)$
$[43]=(H,P,H,P,H,P)$	$[44]=(H,P,H,P,H,H)$	$[45]=(H,P,H,H,P,P)$
$[46]=(H,P,H,H,P,H)$	$[47]=(H,P,H,H,H,P)$	$[48]=(H,P,H,H,H,H)$
$[49]=(H,H,P,P,P,P)$	$[50]=(H,H,P,P,P,H)$	$[51]=(H,H,P,P,H,P)$
$[52]=(H,H,P,P,H,H)$	$[53]=(H,H,P,H,P,P)$	$[54]=(H,H,P,H,P,H)$
$[55]=(H,H,P,H,H,P)$	$[56]=(H,H,P,H,H,H)$	$[57]=(H,H,H,P,P,P)$
$[58]=(H,H,H,P,P,H)$	$[59]=(H,H,H,P,H,P)$	$[60]=(H,H,H,P,H,H)$
$[61]=(H,H,H,H,P,P)$	$[62]=(H,H,H,H,P,H)$	$[63]=(H,H,H,H,H,P)$
$[64]=(H,H,H,H,H,H)$		,

TABLE SIII. The degeneracy of contact energies in $\mathcal{G}_6$

Q_1={$[1]$}	Q_2={$[2]$}	Q_3={$[3],[17]$}
Q_4={$[4],[18]$}	Q_5={$[5]$}	Q_6={$[6],[41]$}
Q_7={$[7],[21]$}	Q_8={$[8],[22],[43],[57]$}	Q_9={$[9]$}
Q_{10}={$[10]$}	Q_{11}={$[11],[25]$}	Q_{12}={$[12],[26]$}
Q_{13}={$[13]$}	Q_{14}={$[14]$}	Q_{15}={$[15],[29]$}
Q_{16}={$[16],[30]$}	Q_{17}={$[19]$}	Q_{18}={$[20]$}
Q_{19}={$[23]$}	Q_{20}={$[24],[59]$}	Q_{21}={$[27]$}
Q_{22}={$[28]$}	Q_{23}={$[31]$}	Q_{24}={$[32]$}
Q_{25}={$[33]$}	Q_{26}={$[34]$}	Q_{27}={$[35],[49]$}
Q_{28}={$[36],[50]$}	Q_{29}={$[37]$}	Q_{30}={$[38]$}
Q_{31}={$[39],[53]$}	Q_{32}={$[40],[54]$}	Q_{33}={$[42]$}
Q_{34}={$[44],[58]$}	Q_{35}={$[45]$}	Q_{36}={$[46]$}
Q_{37}={$[47],[61]$}	Q_{38}={$[48],[62]$}	Q_{39}={$[51]$}
Q_{40}={$[52]$}	Q_{41}={$[55]$}	Q_{42}={$[56]$}
Q_{43}={$[60]$}	Q_{44}={$[63]$}	Q_{45}={$[64]$}

The set $\mathcal{G}_6$ is partitioned into forty-five subsets within which all sequences possess the same energies.

TABLE SIV. Comparison of the protein folding times for the forty-five situations (A)

subset	$\tau_{\rm fd}$	$\tau_{\rm fd}^{\rm c}$	$\tau_{\rm fd}/\tau_{\rm fd}^{\rm c}$	subset	$\tau_{\rm fd}$	$\tau_{\rm fd}^{\rm c}$	$\tau_{\rm fd}/\tau_{\rm fd}^{\rm c}$
Q_1 :	6.013334	136.035087	22.622240	Q_2 :	3.098551	160.247563	51.716936
Q_3 :	3.520525	96.315062	27.358153	Q_4 :	2.967067	112.623345	37.957803
Q_5 :	6.458355	146.705338	22.715589	Q_6 :	2.866759	181.768820	63.405686
Q_7 :	3.392589	103.502335	30.508362	Q_8 :	2.889039	126.895859	43.923207
Q_9 :	6.038505	157.593573	26.098111	Q_{10} :	2.921799	247.545879	84.723788
Q_{11} :	3.327806	110.875024	33.317755	Q_{12} :	2.801380	171.669173	61.280217
Q_{13} :	7.234799	169.607081	23.443233	Q_{14} :	2.946329	275.445274	93.487616
Q_{15} :	3.191671	118.864775	37.242177	Q_{16} :	2.708122	190.313983	70.275262
Q_{17} :	4.216321	68.078909	16.146519	Q_{18} :	4.724344	78.765355	16.672231
Q_{19} :	3.016037	72.794175	24.135704	Q_{20} :	3.612531	87.963045	24.349423
Q_{21} :	3.804250	77.658548	20.413629	Q_{22} :	3.512217	117.651074	33.497667
Q_{23} :	3.396357	82.796081	24.377909	Q_{24} :	3.900503	129.733781	33.260782
Q_{25} :	3.066039	156.489675	51.039688	Q_{26} :	2.388859	202.780028	84.885725
Q_{27} :	2.937746	110.044318	37.458759	Q_{28} :	2.441537	141.135648	57.806066
Q_{29} :	2.869247	210.959777	73.524439	Q_{30} :	2.303083	275.098917	119.448112
Q_{31} :	2.873812	146.665698	51.035244	Q_{32} :	2.232110	189.940402	85.094553
Q_{33} :	2.494938	301.894318	121.002734	Q_{34} :	2.343357	208.004786	88.763593
Q_{35} :	2.752986	237.048877	86.106096	Q_{36} :	5.974401	403.400204	67.521448
Q_{37} :	2.697952	164.314142	60.903286	Q_{38} :	2.304499	277.603821	120.461680
Q_{39} :	3.968589	77.036636	19.411593	Q_{40} :	3.528882	97.314095	27.576466
Q_{41} :	5.378916	100.994382	18.775973	Q_{42} :	3.597822	129.316623	35.943030
Q_{43} :	1.893287	141.255927	74.608830	Q_{44} :	3.922487	112.584764	28.702393
Q_{45} :	1.877747	187.603586	99.908873				

The data in the above is calculated by taking the structure-9 as the target state.

TABLE SV. Comparison of the protein folding times for the forty-five situations (B)

subset	$\tau_{\rm fd}$	$\tau_{\rm fd}^{\rm c}$	$\tau_{\rm fd}/\tau_{\rm fd}^{\rm c}$	subset	$\tau_{\rm fd}$	$\tau_{\rm fd}^{\rm c}$	$\tau_{\rm fd}/\tau_{\rm fd}^{\rm c}$
Q_1 :	3.007868	58.811334	19.552498	Q_2 :	2.479394	56.885456	22.943290
Q_3 :	2.915515	62.760625	21.526428	Q_4 :	2.737002	60.829525	22.224874
Q_5 :	2.662492	61.269774	23.012191	Q_6 :	2.184729	55.766683	25.525675
Q_7 :	2.610164	65.195489	24.977545	Q_8 :	2.355810	59.440630	25.231504
Q_9 :	2.561153	66.410402	25.929885	Q_{10} :	2.121793	80.139792	37.769845
Q_{11} :	2.650392	70.320819	26.532233	Q_{12} :	2.376243	83.876242	35.297839
Q_{13} :	2.298248	55.371229	24.092800	Q_{14} :	1.866984	62.231172	33.332461
Q_{15} :	2.443572	58.510481	23.944652	Q_{16} :	2.099786	65.095912	31.001213
Q_{17} :	3.058518	80.326256	26.263130	Q_{18} :	2.892302	78.325642	27.080727
Q_{19} :	4.049810	82.688870	20.417963	Q_{20} :	3.704805	75.757923	20.448559
Q_{21} :	4.850417	87.771468	18.095654	Q_{22} :	2.640431	100.666945	38.125194
Q_{23} :	2.511114	72.516173	28.878089	Q_{24} :	2.270134	77.941553	34.333459
Q_{25} :	1.352143	61.804911	45.708857	Q_{26} :	2.105304	57.913441	27.508351
Q_{27} :	2.544296	66.400618	26.097835	Q_{28} :	2.252789	63.908920	28.368800
Q_{29} :	1.286258	73.047173	56.790452	Q_{30} :	3.928691	66.756540	16.992057
Q_{31} :	1.301468	77.602514	59.626909	Q_{32} :	3.513602	72.667062	20.681643
Q_{33} :	1.785740	62.875193	35.209601	Q_{34} :	2.030462	67.511972	33.249562
Q_{35} :	4.781740	64.586440	13.506891	Q_{36} :	1.588760	60.753000	38.239256
Q_{37} :	2.076350	68.193510	32.842974	Q_{38} :	6.287673	64.546238	10.265521
Q_{39} :	2.414371	86.787849	35.946360	Q_{40} :	2.252013	90.261891	40.080537
Q_{41} :	2.096400	97.939811	46.718093	Q_{42} :	2.004589	98.749514	49.261726
Q_{43} :	2.138715	88.018182	41.154704	Q_{44} :	2.051656	84.318310	41.097684
Q_{45} :	1.935271	81.391188	42.056739				

The data in the above is calculated by taking the structure-19 as the target state.

TABLE SVI. Comparison of the protein folding times for the forty-five situations (C)

subset	$\tau_{\rm fd}$	$\tau_{\rm fd}^{\rm c}$	$\tau_{\rm fd}/\tau_{\rm fd}^{\rm c}$	subset	$\tau_{\rm fd}$	$\tau_{\rm fd}$	$\tau_{\rm fd}/\tau_{\rm fd}^{\rm c}$
Q_1 :	3.534390	107.326690	30.366397	Q_2 :	3.109753	75.781759	24.369061
Q_3 :	3.676584	115.724340	31.476050	Q_4 :	3.021071	81.647239	27.025925
Q_5 :	1.985434	113.879920	57.357696	Q_6 :	2.996953	81.103898	27.062119
Q_7 :	1.998518	122.248609	61.169631	Q_8 :	2.765095	86.798091	31.390636
Q_9 :	2.896183	73.311216	25.313047	Q_{10} :	6.663490	51.723617	7.762241
Q_{11} :	2.996405	78.338356	26.144115	Q_{12} :	3.925446	54.768113	13.952074
Q_{13} :	2.570879	76.241005	29.655618	Q_{14} :	2.167717	53.557491	24.706865
Q_{15} :	2.865303	81.211569	28.343100	Q_{16} :	2.252009	56.512998	25.094481
Q_{17} :	3.702682	151.733536	40.979359	Q_{18} :	4.962379	106.785040	21.518921
Q_{19} :	2.010765	158.129502	78.641463	Q_{20} :	4.560383	111.178045	24.379103
Q_{21} :	5.453139	99.879543	18.315972	Q_{22} :	4.751003	67.798839	14.270426
Q_{23} :	4.285138	102.503862	23.920784	Q_{24} :	4.327710	69.153246	15.979177
Q_{25} :	1.966476	123.623213	62.865356	Q_{26} :	3.305973	96.940512	29.322838
Q_{27} :	1.992959	133.386930	66.929089	Q_{28} :	2.592900	106.332739	41.009194
Q_{29} :	1.710127	160.168363	93.658753	Q_{30} :	3.101977	124.796863	40.231395
Q_{31} :	1.713752	169.914771	99.147818	Q_{32} :	2.756688	134.294122	48.715749
Q_{33} :	2.157100	60.285284	27.947376	Q_{34} :	7.491422	65.002142	8.676876
Q_{35} :	2.896166	100.987316	34.869312	Q_{36} :	2.057256	73.265667	35.613296
Q_{37} :	2.814767	106.795670	37.941211	Q_{38} :	2.157124	78.093837	36.202757
Q_{39} :	2.008037	175.248216	87.273400	Q_{40} :	4.387504	146.585522	33.409775
Q_{41} :	1.721760	211.679379	122.943604	Q_{42} :	8.130396	174.980161	21.521727
Q_{43} :	7.367946	85.202543	11.563948	Q_{44} :	3.710836	131.651748	35.477652
Q_{45} :	2.161168	98.745327	45.690722				

The data in the above is calculated by taking the structure-20 as the target state.

TABLE SVII. Table of notations

n	number of the amino-acid residues
N_n	total number of protein structure (the lattice conformation)
$\mathcal{S}_n$	the structure set
$\mathcal{G}_n$	the connection graph
Ω_n	the sequence set
a, b, c	index labelling the specific structure, which takes from 1 to N_n
$\mathcal{E}_a^{[\nu]}$	contact energy of the structure s_a, the superscript refers a given sequence $[\nu]$
$\mathcal{E}_{ab}$	the energy difference $\mathcal{E}_{ab} = \mathcal{E}_a - \mathcal{E}_b$
J_{ab}	the elements of adjacency matrix that characterizes the graph $\mathcal{G}_n$
T_{ab}	the elements of the probability transition matrix, $T_{ab} = J_{ab}/\deg(b)$
$\deg(b)$	the degree of vertex-b, $\deg(b) = \sum_a J_{ab}$
L, $L^\dagger$	the Lindblad operator
$[\nu]$	labels for a particular sequence, where ν takes from 1 to 2^n
Q_1, Q_2, etc.	subsets in Ω_n, the contact energies in each subset are degenerate
$\hat{\rho}$	density matrix
ρ_{ab}	the matrix elements of $\hat{\rho}$
p_a	classical probability distributions
$p^{(1)}(t)$, $\hat{\rho}^{(1)}(t)$	the superscript here specifies the initial condition from which the solution is obtained
$P_{a,b}(t)$	probability from structure-a to structure-b at time t
$F_{a,b}(t)$	the first-passage probability from structure-a to structure-b at time t
τ_0	the time period that the first-passage probability vanishes $F_{a,b}(\tau_0) = 0$
$\tau_{\rm fd}$	quantum folding time
$\tau_{\rm fd}^{\rm c}$	classical folding time